ELSEVIER

Image and Vision Computing 19 (2001) 503–516

image AND vision COMPUTING

www.elsevier.com/locate/imavis

Reconstruction of degraded image sequences. Application to film restoration

L. Joyeux, S. Boukir*, B. Besserer, O. Buisson

Laboratoire d'Informatique et d'Imagerie Industrielle (L3i), Université de La Rochelle, Avenue M. Crépeau, F-17042 La Rochelle cedex 1, France

Received 16 April 1999; revised 29 September 2000; accepted 30 September 2000

Abstract

A suitable detection–reconstruction approach is proposed for removing impulsive distortion and other types of deterioration from degraded image sequences. The main application that has motivated this work is the problem of digital film restoration for the movie industry, which has only very recently been explored. Line artifacts, which are prominent degradations in motion picture films, are also considered here. The detection procedure consists of two steps. First, a morphological filter provides impulsive distortions and line scratch candidates. Unlike impulsive distortions, which appear randomly in an image, line artifacts persist in nearby or the same location across several frames. Furthermore, the detection process is complicated by the fact that lines occur as natural part in interesting scenes. Therefore, we add a validation step for separating possible line defects from false detections. It consists in tracking the potential line artifacts over the frames using a Kalman filter. An interpolation technique, dealing with both low and high frequencies around the detected deteriorations, is investigated to achieve a nearly invisible reconstruction of damaged areas.

Keywords: Gray scale morphology; Kalman filter; Tracking; Motion picture restoration

1. Introduction

Within the last decade, the restoration of noisy and noisy–blurred image sequences has become prominent in a large variety of areas like medical imaging, remote surveillance or navigation. The main sources of degradations that can corrupt an image sequence are blurring, white noise and impulsive distortions. The problem of removing such degradations has led to numerous spatio-temporal filters:

- restoring noisy image sequences [7,10,15];
- removing impulsive distortions from an image sequence [1,12,18];
- restoring noisy–blurred image sequences [4,27,32].

In contrast to the work done in noise suppression, there has been a little treatment of the problem of suppressing impulsive distortion in image sequences. The problem is not a negligible one especially in motion pictures showing randomly dispersed bright and dark flashes.

Conventional image sequence restoration algorithms perform some form of global filtering of the frames. Most of the work done to date in the area of impulsive noise suppression in images involves median filtering. The median operation has been quite successful in images since it preserves edges well. However, it tends to homogenize highly textured regions in the image. To alleviate this distortion, the window used for the median filter must be as small as possible (3×3 in general). But, impulsive distortion greater in size than 3×3 cannot be completely removed after one pass. Further passes would remove such distortion but affect the output image quality. To enable greater fidelity to be achieved in the image sequence, the Multilevel Median Filter (MMF) was introduced by Nieminen [26]. This class of filters employs a hierarchy of median operations that allows one to reject impulsive distortions on the image with less smoothing than a simple median operation. Extended versions of MMF have been proposed by Arce [2] and Alp [1].

It would be an improvement to implement these filters along a motion trajectory [14,18,23]. Motion-compensated spatio-temporal filters attempt to take full advantage of the temporal correlation that exists between frames. However, this requires that the displacement field be estimated from a noisy image sequence. Generally, this is treated as a separate step in the filtering process. A major drawback comes from the commonly used assumption that both the displacement and intensity fields are homogeneous. This assumption

* Corresponding author. Tel.: +33-5-4645-8284; fax: +33-5-4645-8242.
E-mail address: samia.boukir@univ-lr.fr (S. Boukir).

0262-8856/01/$ - see front matter
PII: S0262-8856(00)00091-3

Fig. 1. Frame of a film sequence (La belle et la bête, 1946).

can result in severe artifacts (over-smoothing of edges). Furthermore, estimation of the motion from image sequences is, in general, a difficult and time-consuming task. It is also difficult to have an idea of the real sensitivity to noise or to image alteration of a motion estimator.

The probabilistic approach produced better results but at a much higher computational cost [12]. Geman proposed a nonlinear filter designed to remove noise and other types of degradation from single images or temporal sequences while at the same time preserving boundaries and other authentic features of the original scene. Unlike previous spatio-temporal filters, this approach is optimization-based. The processed frame sequence is defined as the minimizer of an image functional rather than as the final result of a series of filters. Spatial and temporal processing are performed at the same time: the brightness value at a pixel in the processed frame reflects a compromise between the values suggested by the spatial neighbors in the same frame and the values suggested by the motion-compensated neighbors in the temporal sequence. However, this method is complex and is often computationally intensive.

For good detail preservation of texture, it is necessary to look beyond the use of global filters, which are applied to the entire image. Areas of the images not affected are often of very high definition and it is thus desirable not to filter these areas, as filtering will inevitably introduce some distortion. For the 1D (audio) case, Veldhuis has presented a successful method, which involves accurate detection of the impulsive distortions followed by the reconstruction of damaged areas [36]. It is an effective way of decreasing computation and increasing output quality. Motivated by the work on audio restoration, Kokaram developed a model-based approach to impulsive distortion removal [18]. The emphasis is then placed on the choice of an adequate mathematical model for the luminance variation to catch a local interaction of some neighbor pixels. One can then develop a method, which fits this form to the observed image. To interpolate known missing areas, polynomial models have been used [21,35]. Polynomial interpolation usually relies on spline or B-spline representations, which are the basis for curve fitting [21]. The only requirement of such methods is the order of the polynomial that best fits the input signal. This is a good solution for the reconstruction of homogeneous regions. However, it fails to reconstruct regions of high activity such as textured areas because it approximates only the low frequencies of the input signal. Stochastic models such as Auto Regressive (AR) models [17,18] or Markov Random Field (MRF) models [22,24] allow a better interpolation than polynomial models. Indeed, the high frequencies, which are lost in polynomial interpolation may be recovered using such stochastic interpolation procedure. However, they are difficult to implement.

Fourier series allow a simple representation of input signals either with low- or/and high-frequency components [3,11]. While polynomial and stochastic models require the knowledge of the model order, the use of Fourier series only depends on the number of samples of the discrete signal. Therefore, we propose a powerful restoration technique, based on Fourier series, providing good detail preservation of texture in degraded image sequences. This two-stage

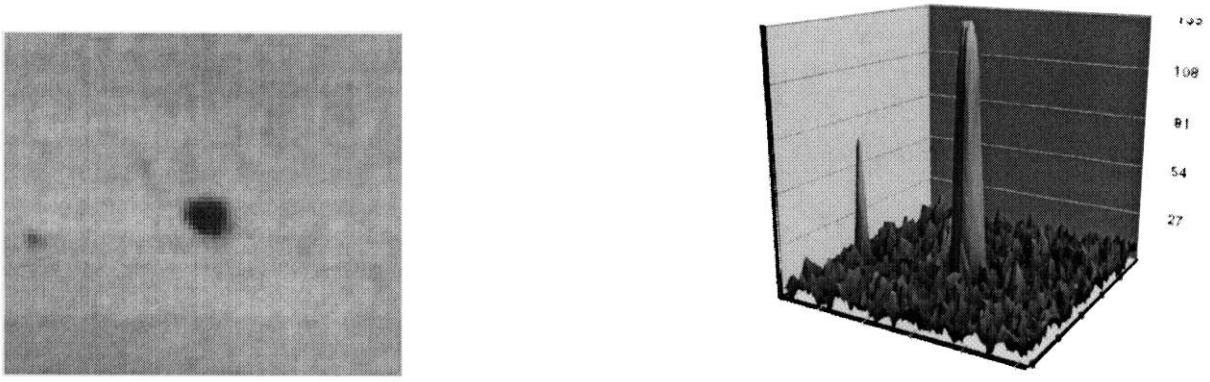

Fig. 2. Image part (left) and corresponding impulsive distortion detection using B_0 (right).

restoration approach first aims at recovering the low-frequency contents and then deals with higher frequency characteristics. Before this, damaged areas are detected using a morphological filter, which incorporates both computational simplicity and good performance.

Unlike the latter model-based restoration approaches, our method is a spatial process. Let us emphasize that spatio-temporal restoration algorithms are more effective than 2D processes only if the motion estimator performs satisfactorily. However, the behavior of a motion estimator cannot be guaranteed. There is also the consideration that the sequences being dealt with are degraded, so the motion estimator must be robust to noise. Furthermore, 3D restoration methods are far more computationally expensive than 2D techniques.

This paper is organized as follows. Section 2 briefly presents the main application that has motivated this work. Section 3 describes the first step of our detection–reconstruction approach; the detection of impulsive distortions using a morphological filter. The same filter is used to detect line artifacts. However, the successful treatment of these defects requires also a tracking process, which is described in Section 4. Section 5 focuses on the reconstruction stage, which relies on both polynomial interpolation and Fourier series. Discussions and concluding remarks are given in Section 6.

2. Problem statement

The application that motivates this work is the restoration of archived black and white motion pictures. Old films are subject to a variety of degradations, which reduce their usefulness. The main visual defects are dust spots due to dust and dirt attached to the film or abrasion removing the emulsion and line scratches due to film slippage during fast start, stops and rewinding, therefore scratching the film with accumulated dirt particles. Fig. 1 shows a frame exhibiting some typical examples of these artifacts.

Digital film restoration has only very recently been explored [8,9,12,18,20,24,29]. Up to now, old films have been restored using traditional film restoration techniques like chemical baths or film polishing. However, such techniques do not permit the removal of all kinds of degradations. Computer-aided techniques have also been used to restore classic old films but they remain very expensive and take several months for the treatment of just one movie. Digital restoration lets us expect results beyond today's limitations (automated processing, correction of photographed dust spots and scratches, removing large defects,…) in far less time than traditional or computer-aided techniques. A significant productivity gain should then be achieved for the motion picture industry.

In contrast to classical image sequence restoration, an automatic digital film restoration system is further complicated by severe constraints:

- The old films must be scanned at high resolutions in order to preserve the definition and the visual quality of the motion picture images. Therefore, each frame is scanned at 2K resolution (2200 pixels × 1640 pixels) in a 12 bits/pixel range.
- The restoration algorithms must also preserve the visual quality of the films.
- The processing power has to be cheap, processing time as short as possible and the restoration process should be automated to cut exploitation costs.

Most existing work on old film restoration is based on the video format [8,9,12,18,20,24,29]. If we apply these techniques on 2K images, they will involve high computational cost. Besides, motion picture (35 mm) images require a much better visual quality than video, thus increasing the complexity of the digital restoration task.

Our digital restoration system automatically detects then corrects artifacts in degraded motion pictures with minimal human intervention. Operator assistance is required mainly to segment the film sequences into sequences of the same scene. Indeed, we do not automatically handle scene

Fig. 3. An ambiguous image part (left) and corresponding impulsive distortion detection (right).

changes. Human supervision is also necessary to tune two external parameters to the detection process and to check the results of this stage before the restoration step. Both detection and correction steps run without human interaction on the raw image sequence while, in computer-aided techniques, the defects are selected then corrected manually, thus requiring a large number of operators and resulting in unacceptably slow process for industrial use.

In this paper, we will mainly focus on the detection and the removal of dust spots and line scratches, which are the most frequent artifacts damaging old films. Of course, the applications of the algorithms presented here are not limited to motion pictures. Similar treatment may be used for any degraded image sequence.

3. Spatial detection of impulsive distortions

Impulsive distortions damaging old films are mainly caused by dust, hair and scratches. They have the following properties:

- The gray levels of these artifacts tend to the black, that means local minima, or to the white, which correspond to local maxima.
- They have strong edges.
- The maximal spatial surface of the in-scope deteriorations is bounded in relationship with the scanning resolution.

Dust spots typically can be found on one frame only and will therefore present a strong temporal discontinuity in image brightness. Some form of temporal filtering that can remove outliers seems an obvious strategy to employ [18,24,34]. However, that motion will need to be compensated for. Unfortunately, motion estimation is not a solved problem and is also the subject of much research. The design of a spatio-temporal algorithm is made difficult by the motion of objects in the scene. Furthermore, it requires high computational cost particularly in the case of 2K images. Therefore, to detect impulsive distortions, we propose a simple spatial method based on morphological filtering.

3.1. Gray scale morphology

The four fundamental binary morphological transformations (erosion, dilation, closing and opening) are all extended to gray scale morphology, without thresholding via the use of local maximum and minimum operations.

Given a gray scale image I and a structuring element B, the following neighborhood operators $\oplus$ and $\ominus$ form the basis of classical mathematical morphology [25,31,33]:

$$\begin{cases} \text{Dilation}: I \oplus B = \text{MAX}_{(u,v)\in B}(I(x+u, y+v) - B(u,v)) \\ \text{Erosion}: I(\ominus)B = \text{MIN}_{(u,v)\in B}(I(x+u, y+v) + B(u,v)) \\ \text{Closing}: I^B = (I \oplus B)\ominus B \\ \text{Opening}: I_B = (I\ominus B) \oplus B \end{cases} \tag{1}$$

3.2. A morphological filter for impulsive distortion detection

The closing operator has the attractive property of deleting local minima. Therefore, we can use it to detect black impulsive distortions. Similarly, the opening operator appears well suited for the detection of white deteriorations. Both morphological detectors of black and white deteriorations are then expressed as a simple difference between the closing (or the opening) and the original image:

$$\begin{aligned} D_{\text{black}}(I(x,y), B) &= ((I(x,y) \oplus B)\ominus B) - I(x,y) \\ D_{\text{white}}(I(x,y), B) &= I(x,y) - ((I(x,y)\ominus B) \oplus B) \end{aligned} \tag{2}$$

Impulsive distortions are then detected when the absolute value of these differences are greater than a predetermined threshold S. This parameter is experimentally fixed by an operator who checks the detection results (image masks) on the first image of the sequence before running the detection process on the whole sequence. If the chosen value is low, the detector reacts to noise; otherwise, the localization of the distortions is imprecise. Let us notice that this parameter

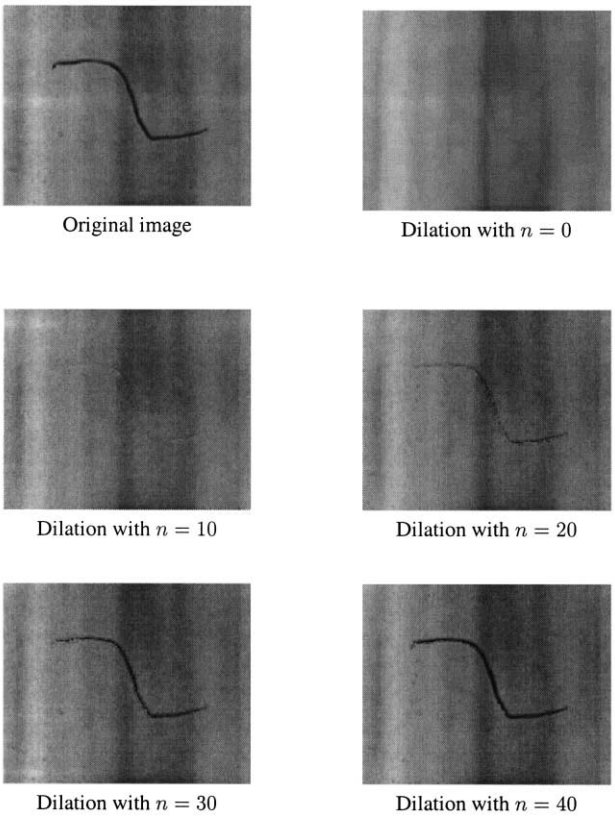

Fig. 4. Effects of parameter n on a dilation operation using B_n.

does not require a fine tuning. The same value, $S = 10$, has been successfully used for all our experiments. Let us emphasize that a detection rate of 90% (with less than 5% of false detections) is sufficient to achieve a suitable visual quality after correction.

3.2.1. Flat structuring element

First, we define a flat structuring element B_0 as a matrix of 9×9 elements whose values have been fixed to zero. The dimensions of the structuring element have been chosen in concordance with the maximal spatial surface of the impulsive defects. The detection of impulsive distortions caused by dust particles in an image part of the "La belle et la bête" film sequence is shown in Fig. 2. Both defects are well detected.

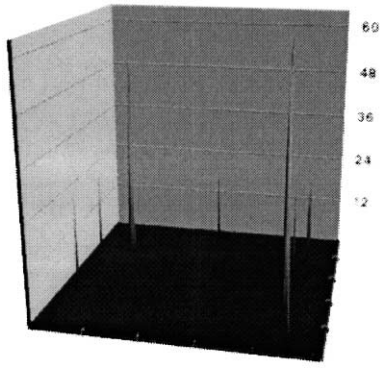

Fig. 5. Impulsive distortion detection using B_{20}.

However, sometimes, this detector selects also natural parts of the image (false detections). Fig. 3 shows another part of the "La belle et la bête" sequence with its resulting deterioration detection. We can notice that, in this second experiment, the defects are hardly distinguishable from their neighborhood.

To handle such ambiguities, we use a new structuring element.

3.2.2. Pyramid-shaped structuring element

We define a new 9×9 structuring element B_n whose values are constrained in order to distinguish between strong edges and smooth ones. This pyramid-shaped structuring element is defined as:

$$B_n = \begin{bmatrix} 4n & 4n & 4n & 4n & 4n & 4n & 4n & 4n & 4n \\ 4n & 3n & 3n & 3n & 3n & 3n & 3n & 3n & 4n \\ 4n & 3n & 2n & 2n & 2n & 2n & 2n & 3n & 4n \\ 4n & 3n & 2n & n & n & n & 2n & 3n & 4n \\ 4n & 3n & 2n & n & 0 & n & 2n & 3n & 4n \\ 4n & 3n & 2n & n & n & n & 2n & 3n & 4n \\ 4n & 3n & 2n & 2n & 2n & 2n & 2n & 3n & 4n \\ 4n & 3n & 3n & 3n & 3n & 3n & 3n & 3n & 4n \\ 4n & 4n & 4n & 4n & 4n & 4n & 4n & 4n & 4n \end{bmatrix} \quad (3)$$

where n represents the slope of image curves gradient.

Only the objects with a slope (at their edges) higher than the parameter n are detected. This is illustrated in Fig. 4, which shows the effects of the parameter n on a simple dilation operation. Indeed, if the slope of the object is lower than n, the object remains as it is. This occurs for $n = 40$; the hair is not dilated. When the slope of the object is greater than n, it is removed. This happens for $n = 10$; the hair is dilated. The parameter n, introduced in our pyramid-shaped structuring element, offers therefore a simple and efficient mean to detect more or less contrasted objects.

Applying B_n ($n = 20$) on the previous critical image, we obtain the result depicted in Fig. 5.

We can point out the significant improvement in the detection accuracy. No ambiguity remains between peaks corresponding to real defects and other peaks. Let us notice that this second parameter to be set in our detection algorithm also does not require a fine tuning. The value we have used in our experiments seems to be a good compromise to detect enough deteriorations with a minimum of false alarms. Indeed, if the image brightness of an object changes of 128 levels per displacement of 4 pixels (near the edge), which is unusual, the slope is 32 and therefore fixing it at 20 appears as a reasonable choice. Let us recall that impulsive

Fig. 6. An image part (left) and corresponding impulsive distortion detection using B_{20} (right).

distortions have usually stronger edges than the objects occurring in interesting scenes.

This morphological filter performs well in the presence of ambiguities. However, it might not reliably detect some deteriorations. Fig. 6 shows an impulsive distortion, due to a hair, extracted from "La belle et la bête" film sequence. We can notice that the resulting defects detection is of poor quality. Therefore, we propose a new detector combining both the flat and the pyramid-shaped structuring elements.

3.2.3. Multiple structuring elements

The basic idea is to simultaneously use the two structuring elements B_0 and B_n in the same detector:

$$D_{\text{black}}(I(x,y), B_0, B_n) = ((((I(x,y) \oplus B_0) \oplus B_n) \ominus B_n) \ominus B_0) - I(x,y) \quad (4)$$

Here B_0 and B_n dimensions have been fixed to 5×5 instead of 9×9 in order to handle defects of same size. Fig. 7 shows the results obtained on images 3 and 6 using this new morphological filter. Both results are very satisfactory and demonstrate the robustness of our impulsive distortion detection method.

Figs. 8 and 9 show the result of our detector on the whole image of "La belle et la bête" frame using $n = 0$ and $n = 20$, respectively. These results clearly demonstrate the usefulness of the slope n to minimize the rate of false detections, which are particularly noticeable on the left-hand side of Fig. 8. More examples are shown in Fig. 10. These results illustrate once again the efficiency of our filter.

The major advantage of our technique over spatio-temporal methods such as those mentioned in Refs. [18,24] or [17] lies in its good computational performance. Indeed, for a 2K image, the detection step is performed in less than 6 s on a conventional workstation. Let us notice that to achieve such a performance, the erosion and dilation operators have been optimized under the application of both the flat and the pyramid-shaped structuring elements [6].

To evaluate the performances of our dust spot detector, a statistical study has been carried out on an undamaged film sequence, which has been artificially deteriorated [5]. This investigation has led to the following detection rates: 1.5% of false detections and 9% of undetected defects. Let us notice that it is obviously preferable to miss a few amount of dust spots than to remove scene features. The false detection rate has then to be as low as possible to preserve the visual quality of the processed movie.

Fig. 7. Impulsive distortion detection using B_0 and B_{20} on image 3 (left) and on image 5 (right).

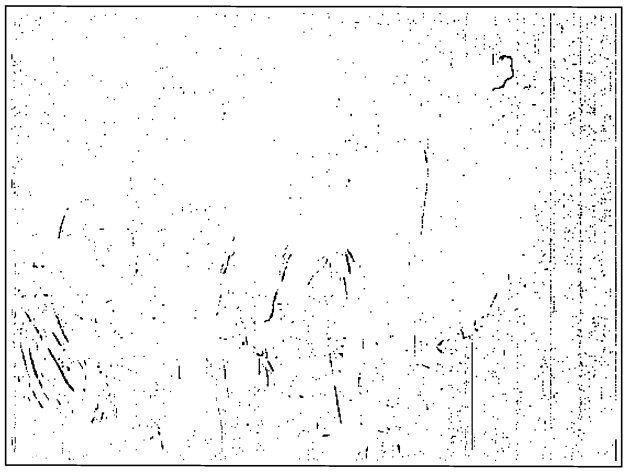

Fig. 8. Impulsive distortion detection on "La belle et la bête" frame ($n = 0$).

In the next section, our morphological filter is also used to detect line scratches. However, we will see that a purely spatial method could not perform a reliable detection of such artifacts because of their frequent occurrence in natural scenes and their persistence over the image sequence. Therefore, we adopt a spatio-temporal method for the detection of such defects.

4. Spatio-temporal detection of line artifacts

While line scratches have the same photometric characteristics as impulsive distortions, their particular shape and their temporal behavior do not allow us to consider them as a subset of impulsive distortions.

Line scratches are easily visible as vertical lines of bright or dark intensity, oriented more or less vertically over much of the image. The length or duration of a line scratch is unknown (less than a frame up to a whole reel) and sometimes periodical, hence detecting the beginning and the trailing of a scratch is a special case. Detection is complicated by the fact that lines occur as natural part in interesting scenes. Furthermore, the defect persists in nearby or the same location across several frames. Thus, detection of line artifacts cannot rely on temporal discontinuity in image brightness.

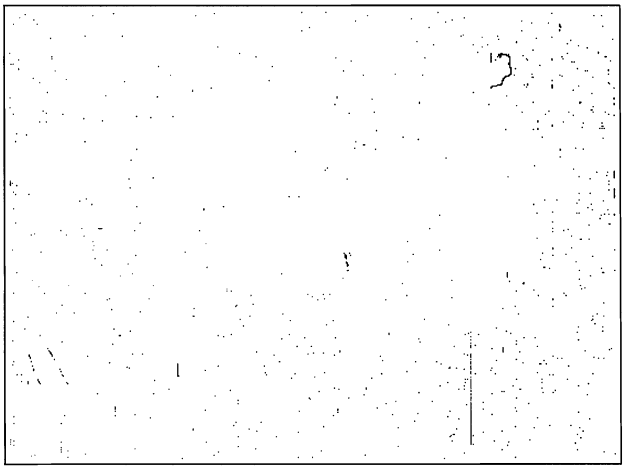

Fig. 9. Impulsive distortion detection on "La belle et la bête" frame ($n = 20$).

Rather than using only one frame to detect line scratches [9,19,24], we focus on temporal features, even for not perfectly vertical line scratches (see Fig. 11). Indeed, one has to check the behavior of potential line artifacts over the film sequence to reject false detections.

4.1. Vertical sub-sampling before detection

A line scratch is a local extremum of the intensity curve along the x-axis. Film grain, dust spots and scanner artifacts introduce noise as shown in Fig. 11. We rely on Radon projections along the y-axis to minimize noise influence [30]. This vertical sub-sampling is a simple and efficient procedure to enhance vertical line features and reduce noise [19,29]. Thus, line artifacts become vertically smooth but remain horizontally impulsive.

Given a gray scale image I, our data projections may be expressed as:

$$\mathscr{P}_H(x,i) = \sum_{j=0}^{H-1} I(x, j + H{\cdot}i) \tag{5}$$

Projection height H is estimated in relation with the greatest acceptable angle to the vertical (less than 5° in practice) and the image resolution. All subsequent work up to the line artifacts detection uses this vertical sub-sampling.

4.2. Spatial detection of line artifacts

Following line scratch features should be extracted from the digital image: location with respect to the x-axis, angle to the vertical, width. Local extrema within each projected strip are detected using our morphological filter described in Section 3.2. The same dimensions (5×5) are used for the two structuring elements. The same threshold, $S = 10$, successfully used for the detection of impulsive defects, is also used here. However, unlike dust spots, line scratches are usually poorly contrasted. Therefore, the slope n has been fixed to zero. Fixing the thresholds at low values allows one to detect every line artifact. However, this also increases the number of wrong detections but the tracking process will eliminate them. Fig. 12 shows, on the top, a frame of "Les allumettes suédoises" video sequence and on the bottom, a sub-sampled sequence of the same film. The result of our spatial line scratch detection algorithm on this sequence is shown on Fig. 13. A great number of false detections is obtained due on the one hand to the use of low thresholds and on the other hand to the high intensity of noise, which makes the detection process very complicated on this film sequence.

In the following, the temporal behavior of the detected

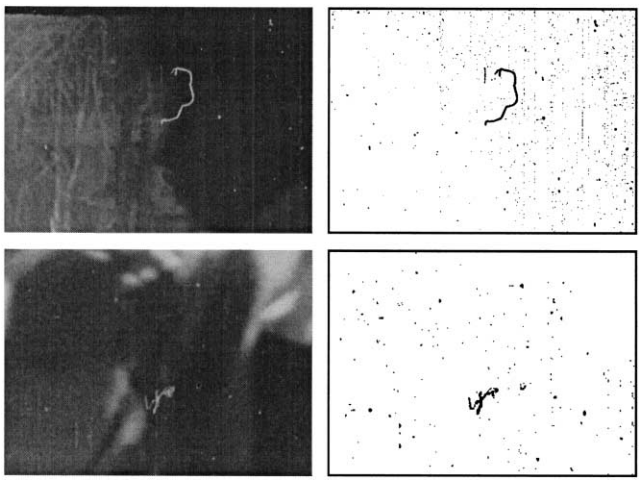

Fig. 10. More examples of impulsive distortion detection.

artifacts will be checked to reject lines occurring as a natural part of the images. Of course, only potential line scratches will be tracked. Small edge chains, under 4-pixel-height stripes (64 pixels), are discarded. Edge chains, which are not vertically oriented (with a tolerance of 5°) are also rejected. Both conditions are in concordance with the line scratch features.

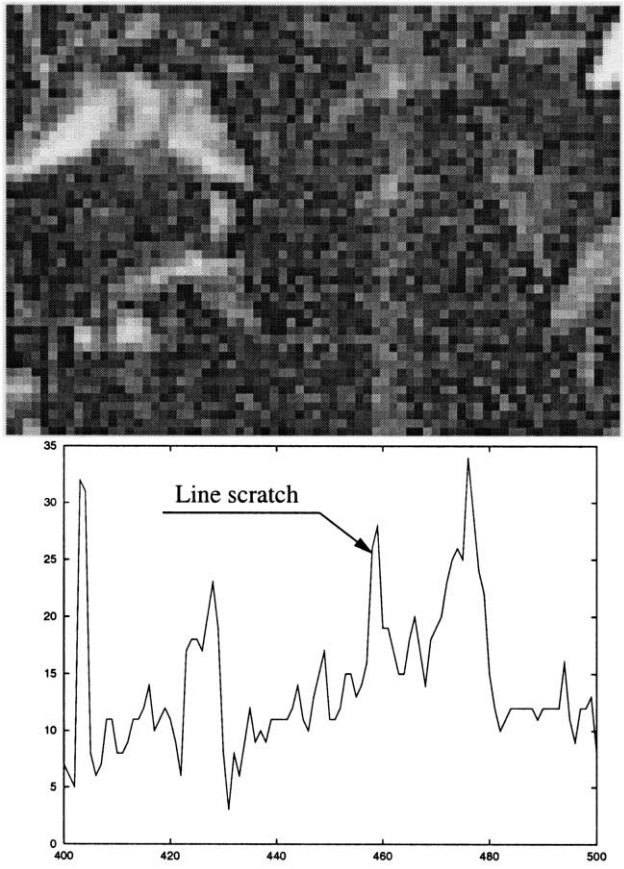

Fig. 11. Enlarged part of a frame. Noise is visible. Below, corresponding line scratch profile.

Fig. 12. Frame of "Les allumettes suédoises" video sequence (720 × 576). Below, sub-sampled sequence (10 frames with 16 pixel-height stripes) of the same film.

4.3. Refinement using Kalman filtering

In this section, we aim at tracking the detected line artifacts over the image sequence to refine the previous spatial detection process. An accurate detection field must be achieved to allow a suitable reconstruction of the deteriorated areas. Indeed, the first detection step only provides an approximate detection field, which may contain false detections. A powerful technique for tracking in this context is the Kalman filter [13,37].

4.3.1. Kalman filter

The Kalman filter is a Bayesian estimation technique used to track stochastic dynamic systems. The filter is based on two probabilistic models:

- The system model, which describes the evolution over time of the current state vector u_k. The transition between states is characterized by the known transition matrix Φ_k

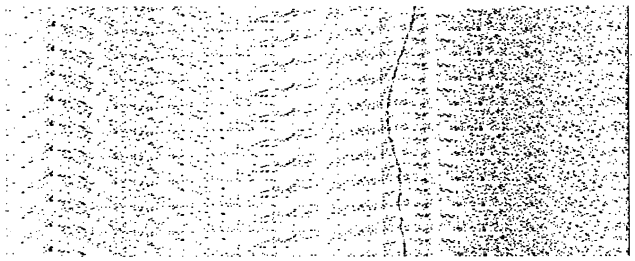

Fig. 13. Line scratch detection on "Les allumettes suédoises" sub-sampled sequence.

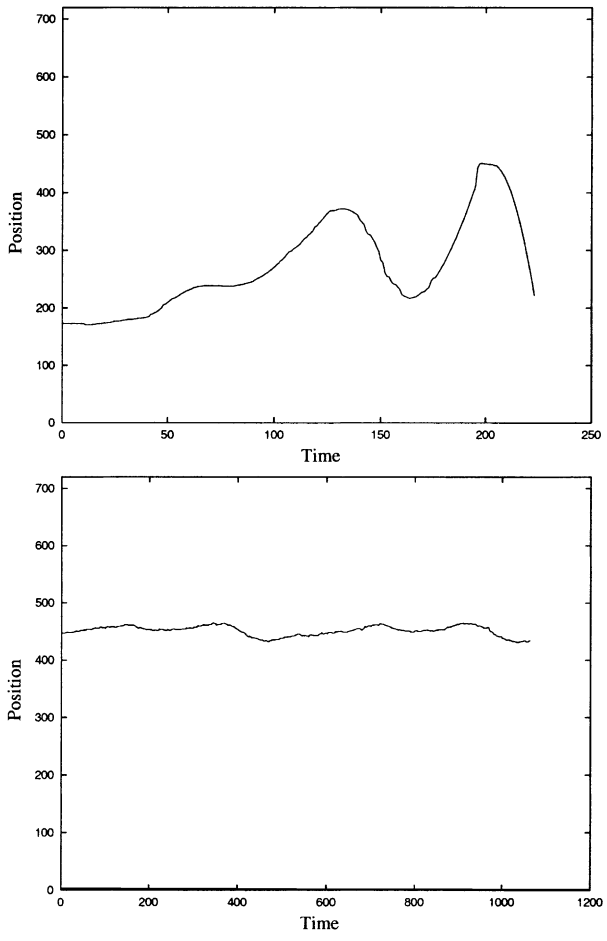

Fig. 14. Line scratch tracking over 30 frames (left). False detection behavior (right). Units along the x-axis are pixels, along the time axis projected stripes.

and the addition of Gaussian noise with a covariance Q_k.

- The measurement model, which relates the measurement vector d_k to the current state through a measurement matrix H_k and the addition of Gaussian noise with a covariance R_k:

$$\begin{cases} u_k = \Phi_k u_{k-1} + \eta_k, & \eta_k \sim N(0, Q_k) \\ d_k = H_k u_k + \xi_k, & \xi_k \sim N(0, R_k) \end{cases} \tag{6}$$

Kalman filter algorithm operates in two phases: prediction and update. The prediction step consists in a state estimate extrapolation and a state covariance extrapolation:

$$\begin{aligned} \hat{u}_{k/k-1} &= \Phi_{k-1}\hat{u}_{k-1/k-1} \\ \hat{P}_{k/k-1} &= \Phi_{k-1}\hat{P}_{k-1/k-1}\Phi_{k-1}^{\mathrm{T}} + Q_{k-1} \end{aligned} \tag{7}$$

Then, the predicted covariance is used to compute a new Kalman gain matrix K_k. Finally, both current covariance matrix and current state are updated:

$$\begin{aligned} K_k &= \hat{P}_{k/k-1}H_k^{\mathrm{T}}[H_k\hat{P}_{k/k-1}H_k^{\mathrm{T}} + R_k]^{-1} \\ \hat{u}_{k/k} &= \hat{u}_{k/k-1} + K_k[d_k - H_k\hat{u}_{k/k-1}] \\ \hat{P}_{k/k} &= (I - K_kH_k)\hat{P}_{k/k-1} \end{aligned} \tag{8}$$

The recursive process is initialized by $\hat{u}_0$, an initial estimate of u and P_0, its error covariance matrix.

4.3.2. Line scratch tracking

The first thing to specify when designing the Kalman filter is the representation used for the state vector [13,37]. In our case, the state vector is related to the position $x(t)$ of the vertical artifact lines over time.

Line scratches are usually generated by rubbing against rotating mechanical pieces. Therefore, they would have a sinusoidal evolution over the image sequence. Classical representation of a sinusoid is: $x(t) = A\sin(\omega t + \varphi)$. To involve Kalman filtering, we use a linear approximation of this model:

$$x(t) = A\left[b(t + c) - \frac{1}{3!}b^3(t + c)^3\right] \tag{9}$$

which is based on the well-known linear approximation of a sine curve expressed at the third order:

$$\sin(x) \simeq x - x^3/3!, \qquad x \to 0 \tag{10}$$

Therefore, the state vector of our line artifact tracking system is: $u_k = (\,a_0 \quad a_1 \quad a_2 \quad a_3)^{\mathrm{t}}$ where a_0, a_1, a_2 and a_3 denote the coefficients of our cubic polynomial model derived from Eq. (9). The expression of the next state $x(t + \mathrm{d}t)$ leads to the following transition matrix:

$$\Phi_k = \begin{pmatrix} 1 & \mathrm{d}t & \mathrm{d}t^2 & \mathrm{d}t^3 \\ 0 & 1 & 2\mathrm{d}t & 3\mathrm{d}t^2 \\ 0 & 0 & 1 & 3\mathrm{d}t \\ 0 & 0 & 0 & 1 \end{pmatrix} \tag{11}$$

The starting state vector is:

$$u_0 = (\,r_0 \quad 0 \quad 0 \quad 0)^{\mathrm{t}} \tag{12}$$

with r_0 being the initial position of the detected line scratch.

The covariance matrices are initialized as follows [16]:

$$Q_0 = (1 \quad 0 \quad 0 \quad 10^{-\rho})^{\mathrm{t}} \qquad R_0 = w_0 \tag{13}$$

with ρ being a convergence factor and w_0 the initial width of the line scratch.

The state covariance matrix coefficients have been initialized to zero.

The Kalman-based tracking process then provides the trajectories of the potential detected line artifacts. The examination of the obtained trajectories easily permits one to distinguish between effective line artifacts (see the left profile on Fig. 14) and false detections (right profile in

Fig. 15. Impulsive distortion removal on "La belle et la bête" frame.

Fig. 14). Let us point out that the latter case may not occur in practice because the tracking of the corresponding line would be interrupted after a few iterations with regard to its incompatible behavior with respect to a line artifact trajectory. Such a false detection behavior is shown to better illustrate the difference between line artifacts and false candidate profiles.

Finally, let us emphasize that our spatio-temporal line scratch detector is a fast process: 10 s/video image (about 20 s/motion picture image).

4.3.3. Discussion

While the digital film restoration system might be tolerant up to 5% of false detections in case of impulsive defects, this tolerance is unacceptable in case of line scratches. Indeed, the removal of significant scene details would have disastrous consequential effects on the resulting restored movie. Human intervention is therefore indispensable to check the line scratch detection results prior to the final restoration stage. Let us emphasize that the rate of undetected line artifacts must be close to zero while a tolerance up to 10% would be acceptable in case of impulsive distortions.

5. Impulsive distortion removal

This stage consists in post-processing the detection field. To reconstruct the corrupted pixels of the detected impulsive distortions, we use an interpolation method [17,20,22,24,35,36]. Classical image interpolation procedures fall into three main categories: intensity-based, contour-based and shape-based interpolations. In our case, we involve an intensity-based interpolation. This technique takes the original pixel intensity value and generates a new interpolated pixel intensity. The calculation of the interpolated value takes a limited number of data points within a small neighborhood. Two kinds of neighborhood may then be used:

- a spatial neighborhood extracted from the current frame;
- a spatio-temporal neighborhood extracted from the current image and the preceding and/or the following frames of the sequence.

As computing power is an important factor for old film restoration, we use a spatial neighborhood around the artifacts. Let us notice that as the size of the considered impulsive distortions is limited to a few pixels, using only the pixels surrounding these deteriorations in the current frame seems to be sufficient for efficient interpolation. Of course, this spatial restoration technique may easily be extended to a spatio-temporal process if the motion is compensated for. However, this will induce higher computational cost mainly caused by the motion analysis stage.

5.1. A two-stage restoration method

The aim here is to produce as seamless a restoration as possible. To completely remove the detected artifacts, we propose a two-stage restoration approach, which first reconstructs low-frequency components and then deals with higher frequencies. Thus, our technique provides the user with a choice to select explicitly the restoration quality: moderate quality with the first restoration step, high quality with an additional step. Off course, there is a trade-off between the desired restoration quality and the processing speed.

5.1.1. Low-pass image reconstruction

Classical methods such as low-pass filters [12] or median filters [1,18,26,28] are not appropriate tools for high-quality restoration because they deteriorate high-frequency components of the images. Our low-pass image reconstruction method is a polynomial interpolation based on a cubic polynomial:

$$I_{\mathrm{LP}}(x,y) = \sum_{k=0}^{3}\sum_{l=0}^{3} a_{kl}x^k y^l \tag{14}$$

which is the most simple model to approximate low-frequency components of an image.

To estimate the model coefficients a_{kl}, we use a least-squares technique whose input data are the coordinates (x_i,y_i) of uncorrupted pixels P_i belonging to a pixel block $\mathcal{P}$ around the defect.

The resulting estimates $\hat{a}_{kl}$ are then used to reconstruct low-frequency components of the distortion area using

$$R_{\mathrm{LP}}(x_j,y_j) = \sum_{k=0}^{3}\sum_{l=0}^{3} \hat{a}_{kl}x_j^k y_j^l, \qquad (x_j,y_j) \in \mathcal{Q} \tag{15}$$

where $\mathcal{Q}$ denotes the set of deteriorated pixels to reconstruct.

Our low-pass reconstruction method yields impressive results on "La belle et la bête" frame exhibited in Fig. 15.

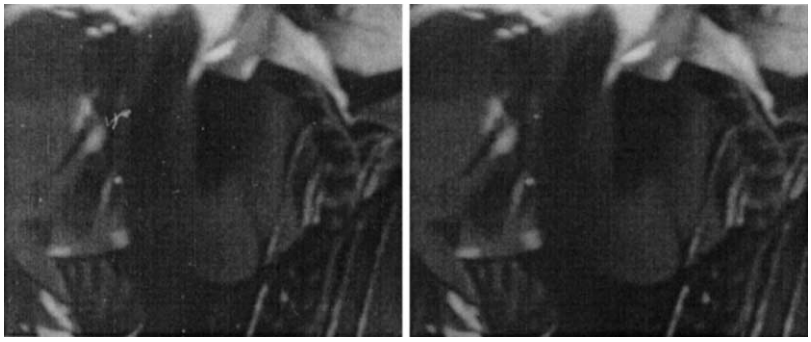

Fig. 16. Part of frame 25 of "La belle et la bête" sequence before and after correction.

We can notice that most impulsive distortions are removed leaving non-degraded areas of the frame untouched. Other results are also depicted in Figs. 16 and 17. However, the restoration is not as seamless in the case of line artifacts. Due to their very strong structure and effect on the appearance of the frame, a high-quality restoration is necessary. Fig. 18 shows, on the left, an image part of a damaged "Frères Lumière" film sequence and, on the middle, the result of our low-pass reconstruction technique on the detected line scratch. We can easily notice the perceived visibility of the interpolated line area. This phenomenon would be emphasized in a film sequence. This shows that a suitable old film restoration process must integrate a method of dealing with high-frequency components (i.e. film grain), which as expected, have been lost in the present case.

5.1.2. High-pass image reconstruction

Numerous image restoration techniques exist but most of them do not or just partially deal with the high frequencies of the images. Very little research work has been devoted to this issue [36]. Furthermore, they are mainly based on the video format [17,20,24].

We propose a high-pass image reconstruction technique based on Fourier series. First, we extract the high frequencies from the area (pixel bloc $\mathscr{P}$), which has been used for the reconstruction of the low frequencies of the degraded region. This is achieved with a simple difference:

$$I_{\mathrm{HP}}(x_i, y_i) = I(x_i, y_i) - I_{\mathrm{LP}}(x_i, y_i), \qquad (x_i, y_i) \in \mathscr{P} \tag{16}$$

Fourier series are well suited for the representation of high frequencies of image profiles. Therefore, our interpolation method relies on the following model:

$$I_{\mathrm{HP}}(x, y) = \sum_{k=0}^{N_{wx}} \sum_{l=0}^{N_{wy}} [a_{kx} \sin(\omega_{kx} x) + b_{kx} \cos(\omega_{kx} x)] \times [a_{ky} \sin(\omega_{ky} y) + b_{ky} \cos(\omega_{ky} y)] \tag{17}$$

where ω_{kx} and ω_{ky} represent the different frequencies of the model.

To illustrate our estimation method of the model coefficients a_{kx}, b_{kx}, ω_{kx}, a_{ky}, b_{ky} and ω_{ky}, let us consider the case of one-dimensional signals. The method may then easily be extended to two-dimensional ones. An input signal $S(x)$ may be represented using Fourier series as:

$$S(x) = \sum_{k=0}^{N_w} a_k \sin(\omega_k x) + b_k \cos(\omega_k x) \tag{18}$$

Assuming $S(x)$ sampled at a constant period in an interval $[0,x_n]$, the model frequencies ω_k can be expressed as: $\omega_k = 2\pi k/x_n$, $k \in [0, x_n - 1]$. To estimate the model coefficients a_k, b_k and ω_k, we use an iterative scheme based on the

Fig. 17. Part of frame 45 of "La belle et al bête" sequence before and after correction.

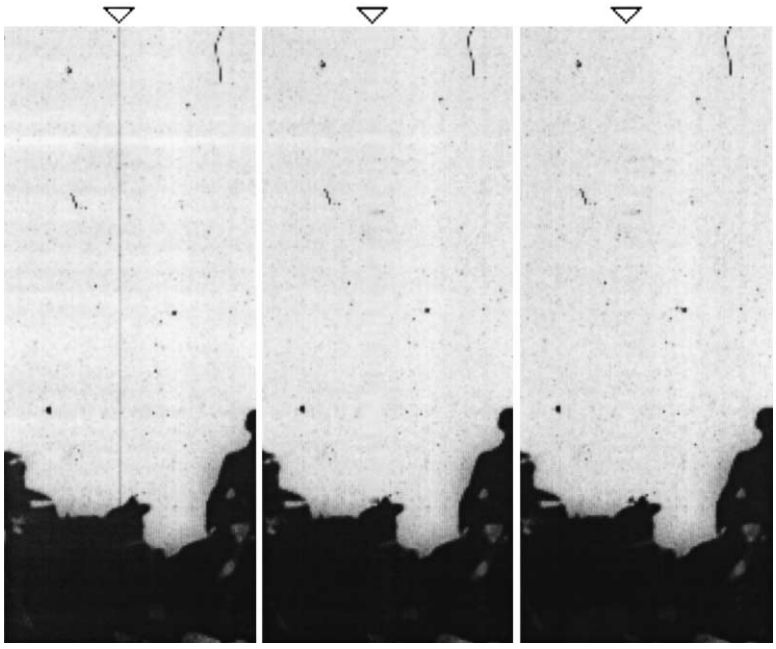

Fig. 18. Frame of a “Frères Lumière” film sequence (left), corresponding low-frequency reconstruction (middle) and low and high frequency reconstruction (right).

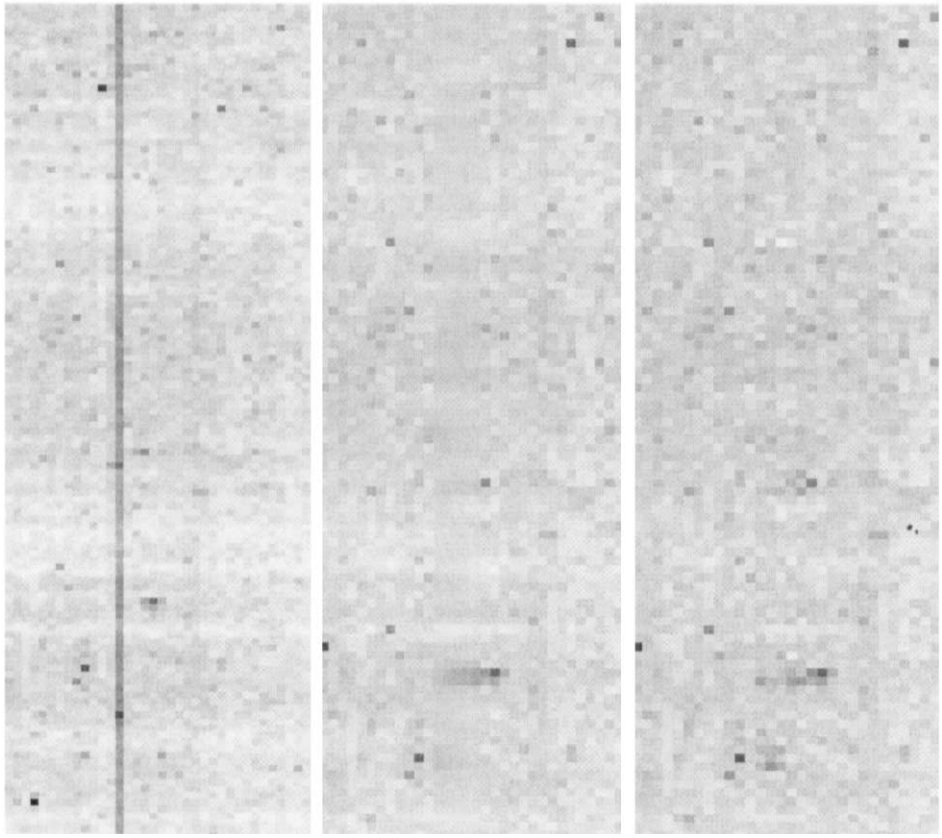

Fig. 19. Enlarged part of the previous original image before restoration (left), after low-frequency reconstruction (middle) and after low- and high-frequency reconstruction (right).

minimization of the following criterion:

$$E(a_k, b_k, \omega_k) = \sum_{x_i \in \mathscr{P}} [a_k \sin(\omega_k x_i) + b_k \cos(\omega_k x_i) - S_k(x_i)]^2 \tag{19}$$

The first step of our incremental algorithm consists in estimating the coefficients a_0, b_0 and ω_0 using the model:

$$S_0(x_i) = a_0 \sin(\omega_0 x_i) + b_0 \cos(\omega_0 x_i), \qquad x_i \in \mathscr{P} \tag{20}$$

Assuming $S_0(x_i) = S(x_i)$, $x_i \in \mathscr{P}$, a Fourier transform of the signal $S_0(x)$ provides an estimation of the frequency ω_0. Then, a least-squares technique, derived from Eq. (20) is used to compute the two other model coefficients. The second stage of our method relies on the decomposition of the signal $S_0(x)$ as:

$$S_1(x_i) = S_0(x_i) - [\hat{a}_0 \sin(\hat{\omega}_0 x_i) + \hat{b}_0 \cos(\hat{\omega}_0 x_i)], \qquad x_i \in \mathscr{P} \tag{21}$$

This process is repeated until the value of criterion $E(\hat{a}_k, \hat{b}_k, \hat{\omega}_k)$ falls under a threshold.

A similar procedure is used to estimate the image model coefficients $\hat{a}_{kx}$, $\hat{b}_{kx}$, $\hat{\omega}_{kx}$, $\hat{a}_{ky}$, $\hat{b}_{ky}$ and $\hat{\omega}_{ky}$. Therefore, the high-frequency components of the distortion area may be reconstructed. The resulting reconstructed signal $R_{\mathrm{HP}}(x_j, y_j), (x_j, y_j) \in \mathscr{Q}$, is then added to the previously computed low-frequency signal $R_{\mathrm{LP}}(x,y)$ to complete our two-stage reconstruction process. Fig. 18 shows, on the right, the result of such restoration method, which produces significant improvement in quality. Some attempt to better illustrate the difference between the low-pass interpolation and the two-stage reconstruction technique is shown in enlarged parts of previous frames (Fig. 19). At that scale, the low-frequency interpolation shows a visibly different area (middle) while the low- and high-frequency restorations do not suffer at all from this over-smoothing phenomenon. This result clearly shows the important reduction of the visibility of the interpolated area and demonstrates that our method is an efficient way of removing distortions from degraded image sequences.

6. Summary and conclusion

We have presented an efficient detection–reconstruction approach for degraded image sequence restoration. The main philosophy in detection is to restrict the attention of the filtering mechanism only to the distorted areas thus leaving non-degraded areas of the frame untouched. A new morphological filter, which incorporates both computational simplicity and good performance, has been introduced. The structuring elements are simple (flat or pyramid-shaped) but are well-suited for the detection of impulsive distortion. This purely spatial method is also used to detect line scratches, which are common artifacts in degraded motion picture films. To separate possible line artifacts from false detections, the potential scratches are tracked over the frames using a Kalman filter. The reconstruction of the detected damaged areas is then performed using a new scheme for detail preserving interpolation. This distortion removal algorithm is a two-stage interpolation technique. The low frequencies of the deteriorated areas are first reconstructed using a simple polynomial interpolation. Then, we deal with the higher frequencies using an appropriate model for such interpolation: Fourier series. This interpolation turned out to be a powerful method leading to a nearby invisible restoration.

Acknowledgements

This work is supported by CENTRIMAGE (Laboratories Neyrac Films — Citélab), Paris, France, under contract C58.

References

[1] B. Alp, et al., Median-based algorithms for image sequence processing, SPIE Visual Communications and Image Processing (1990) 122–133.
[2] G.R. Arce, E. Malaret, Motion preserving ranked-order filters for image sequence processing, IEEE International Conference on Circuits and Systems, 1989, pp. 983–986.
[3] D.H. Bailey, P.H. Swarztrauber, The fractional Fourier transform and applications, SIAM Review 33 (3) (1991) 389–404.
[4] J.C. Brailean, Simultaneous recursive displacement estimation and restoration of noisy-blurred image sequences, IEEE Transactions on Image Processing 4 (9) (1995).
[5] O. Buisson, Analyse de séquences d'images haute résolution, Application à la restauration numérique de films cinématographiques, PhD thesis, Université de La Rochelle, 1997.
[6] O. Buisson, B. Besserer, S. Boukir, F. Helt, Deterioration detection for digital film restoration, CVPR'97, International Conference on Computer Vision and Pattern Recognition, Puerto Rico, USA, vol. 1, June 1997, pp. 78–84.
[7] C.L. Chan, et al., Image sequence filtering in quantum-limited noise with applications to low-dose fluoroscopy, IEEE Transactions on Medical Imaging 12 (3) (1993) 620–621.
[8] M.N. Chong, S. Kalra, D. Krishnan, A. Laud, Computerized motion picture restoration system, Proceedings of BroadcastAsia98, 1998, pp. 153–159.
[9] E. Decencière Ferrandière, Restauration automatique de films anciens, PhD thesis, Ecole Nationale Supérieure des Mines de Paris, 1997.
[10] E. Dubois, S. Sabri, Noise reduction in image sequences using motion-compensated temporal filtering, IEEE Transactions on Communications COM-32 (7) (1984) 826–831.
[11] R.E. Edwards, Fourier Series, 2nd ed., Springer, Berlin, 1982.
[12] S. Geman, D.E. McClure, A nonliner filter for the film restoration and other problems in image processing, Graphical Models and Image Processing (1992) 4.
[13] B. Giai-Checa, R. Deriche, T. Viéville, O. Faugeras, Tracking segments in a monocular sequence of images, Technical Report, INRIA, 1993.
[14] T.S. Huang, Image Sequence Analysis, Springer, Berlin, 1981.
[15] T.S. Huang, Image Sequence Processing and Scene Analysis, vol. 7, Springer, New York, 1983 (COM-32).
[16] L. Joyeux, Reconstruction de séquences d'images haute résolution, Application à la restauration de films cinématographiques, PhD thesis, Université de La Rochelle, France, January 2000.

[17] S. Kalra, M.N. Chong, D. Krishnan, A new auto-regressive (AR) model-based algorithm for motion picture restoration, ICASSP'97, International Conference on Acoustics, Speech and Signal Processing, vol. 4, 1997.
[18] A.C. Kokaram, Motion picture restoration, PhD thesis, University of Cambridge, May 1993.
[19] A.C. Kokaram, Detection and removal of line scratches in degraded motion picture sequences. Signal Processing VIII: Theories and Application, Proceedings of EUSIPCO-96, Trieste, Italy, 1996.
[20] A.C. Kokaram, S.J. Godsill, A system for reconstruction of missing data in image sequences using sampled 3D AR models and MRF motion priors, ECCV'96, European Conference on Computer Vision, vol. 2, 1996, pp. 613–624.
[21] C.H. Lee, Restoring spline interpolation of CT images, IEEE Transactions on Medical Imaging (3) (1983) 142–149.
[22] S.Z. Li, K.L. Chan, H. Wang, Bayesian image restoration and segmentation by constrained optimization, CVPR'96, International Conference on Computer Vision and Pattern Recognition, 1996, pp. 1–6.
[23] D.M. Martinez, Model-based motion estimation and its application to restoration and interpolation of motion pictures, PhD thesis, Massachussetts Institute of Technology, 1986.
[24] R.D. Morris, Image sequence restoration using Gibbs distributions, PhD thesis, University of Cambridge, 1995.
[25] S. Mueller, B. Nickolay, Morphological image processing for the recognition of surface defects. Proceedings of the SPIE, 2249-58, 1994, pp. 298–307.
[26] Nieminen, et al., A. new class of detail-preserving filters for image processing, IEEE Transactions on PAMI (9) (1987) 74–90.
[27] M.K. Ozkan, et al., Efficient multiframe Wiener restoration of blurred and noisy image sequences, IEEE Transactions on Image Processing 1 (1992) 453–476.
[28] I. Pitas, A.N. Venetsanopoulos, Nonlinear Digital Filters. Principles and Applications, Kluwer Academic, Dordrecht, 1990.
[29] L. Rosenthaler, A. Wittmann, A. Günzl, R. Gschwind, Restoration of old movie films by digital image processing, IMAGE'COM 96, Bordeaux, France, May 1996, pp. 1–6.
[30] J.L.C. Sanz, E.B. Hinkle, A.K. Jain, Radon and Projection, Transform-Based, Computer Vision, Springer, Berlin, 1987.
[31] J. Serra, Image Analysis and Mathematical Morphology, Academic Press, London, 1982.
[32] M. Sezan, et al., Motion-compensated multiframe Wiener restoration of blurred and noisy image sequences, IEEE ICASSP 3 (1992) 293–296.
[33] S. Stenberg, Grayscale morphology, Computer Graphics and Image Processing 35 (1986) 333–335.
[34] D. Suter, P. Richardson, Historical film restoration and video coding, Proceedings of PCS'96, Melbourne, 1996, pp. 384–396.
[35] M. Unser, et al., Fast B-spline transforms for continuous image representation and interpolation, IEEE Transactions on Pattern Analysis and Machine Intelligence 13 (3) (1991) 277–285.
[36] R. Veldhuis, Restoration of Lost Samples in Digital Signals, Prentice Hall, Englewood Cliffs, NJ, 1990.
[37] G. Welch, G. Bishop, An introduction to the Kalman filter, Technical Report, University of North Carolina at Chapel Hill, 1997.